Cancer Research

Epigenetic Silencing of miR-137 Is an Early Event in Colorectal Carcinogenesis

Francesc Balaguer[1,2], Alexander Link[1,5], Juan Jose Lozano[3], Miriam Cuatrecasas[4], Takeshi Nagasaka[6], C. Richard Boland[1], and Ajay Goel[1]

Abstract

Global downregulation of microRNAs (miRNA) is a common feature in colorectal cancer (CRC). Whereas CpG island hypermethylation constitutes a mechanism for miRNA silencing, this field largely remains unexplored. Herein, we describe the epigenetic regulation of miR-137 and its contribution to colorectal carcinogenesis. We determined the methylation status of miR-137 CpG island in a panel of six CRC cell lines and 409 colorectal tissues [21 normal colonic mucosa from healthy individuals (N-N), 160 primary CRC tissues and their corresponding normal mucosa (N-C), and 68 adenomas]. TaqMan reverse transcription-PCR and *in situ* hybridization were used to analyze miR-137 expression. *In vitro* functional analysis of miR-137 was performed. Gene targets of miR-137 were identified using a combination of bioinformatic and transcriptomic approaches. We experimentally validated the miRNA:mRNA interactions. Methylation of the miR-137 CpG island was a cancer-specific event and was frequently observed in CRC cell lines (100%), adenomas (82.3%), and CRC (81.4%), but not in N-C (14.4%; $P < 0.0001$ for CRC) and N-N (4.7%; $P < 0.0001$ for CRC). Expression of miR-137 was restricted to the colonocytes in normal mucosa and inversely correlated with the level of methylation. Transfection of miR-137 precursor in CRC cells significantly inhibited cell proliferation. Gene expression profiling after miR-137 transfection discovered novel potential mRNA targets. We validated the interaction between miR-137 and *LSD-1*. Our data indicate that miR-137 acts as a tumor suppressor in the colon and is frequently silenced by promoter hypermethylation. Methylation silencing of miR-137 in colorectal adenomas suggests it to be an early event, which has prognostic and therapeutic implications. *Cancer Res; 70(16); 6609–18. ©2010 AACR.*

Introduction

microRNAs (miRNA) are involved in the pathogenesis of multiple types of cancers, including CRC (1, 2). Growing evidence suggests that miRNAs can act as oncogenes (*onco*miR) or tumor suppressor genes (*ts*miR), and they are involved in the early stages of carcinogenesis (2). The pattern of miRNA expression can be used to classify diverse types and subtypes of cancers (1, 3), and miRNA expression profiles can have prognostic and therapeutic implications (4). Compared with mRNA, a modest number of miRNAs might be sufficient for clinical purposes, and more interestingly, miRNAs remain largely intact in different tissues and are virtually unaffected by RNA degradation (5). All these features make miRNAs a very exciting and promising tool for early tumor detection, prognostication, and treatment.

The causes of the widespread differential expression of miRNAs between tumor and normal cells are still unclear. Approximately 20% of all miRNAs are embedded within CpG islands, and pharmacologic unmasking of silenced miRNAs using epigenetic drugs has revealed that several miRNAs can be inactivated by this mechanism in CRC cell lines (6–8). These studies have permitted the identification of miRNAs that are methylation-silenced in CRC patients (7, 9–11); however, the concept of epigenetic regulation of miRNAs in colorectal carcinogenesis remains largely unexplored.

miR-137 is one such miRNA, which is located on chromosome 1p22 within the non–protein-coding RNA gene AK094607 (12). This miRNA is embedded in a CpG island and is frequently silenced by methylation in several tumors (9, 13, 14). Ectopic transfection of the miR-137 precursor in

Authors' Affiliations: [1]Department of Internal Medicine, Division of Gastroenterology, Charles A. Sammons Cancer Center and Baylor Research Institute, Baylor University Medical Center, Dallas, Texas; [2]Department of Gastroenterology, Institut de Malalties Digestives i Metabòliques, Hospital Clínic, Centro de Investigación Biomédica en Red de Enfermedades Hepáticas y Digestivas (CIBEREHD), IDIBAPS, University of Barcelona; [3]Plataforma de Bioinformática, CIBEREHD; [4]Department of Pathology, Centre de Diagnòstic Biomèdic, Hospital Clínic, IDIBAPS, University of Barcelona, Barcelona, Catalonia, Spain; [5]Department of Gastroenterology, Hepatology and Infectious Diseases, Otto-von-Guericke University, Magdeburg, Germany; and [6]Department of Gastroenterological Surgery and Surgical Oncology, Graduate School of Medicine Dentistry and Pharmaceutical Sciences, Okayama University, Okayama, Japan

Note: Supplementary data for this article are available at Cancer Research Online (http://cancerres.aacrjournals.org/).

Corresponding Authors: Ajay Goel or C. Richard Boland, Gastrointestinal Cancer Research Laboratory, Baylor University Medical Center, 3500 Gaston Avenue, Suite H-250, Dallas, TX 75246. Phone: 214-820-2692; Fax: 214-818-9292; E-mail: ajay.goel@baylorhealth.edu or rickbo@baylorhealth.edu.

doi: 10.1158/0008-5472.CAN-10-0622

oral cancer and glioblastoma multiforme inhibited cell growth, suggesting its tumor-suppressive activity (13, 14). However, the biological role of miR-137 as well as its specific downstream mRNA targets in colorectal carcinogenesis remains unknown. In addition, there are essentially no data about miR-137 disruption in adenomas, the precursor lesion of CRC. We have for the first time systematically characterized the role of miR-137 in the colon by addressing some of the issues mentioned above. We investigated the epigenetic regulation of miR-137 in a panel of six CRC cell lines and more than 400 colorectal tissues, which include both colorectal adenomas and cancers. We explored the tumor-suppressive features of miR-137 *in vitro* and identified potential mRNA targets using whole genome expression profiling. In addition, we have successfully validated *LSD1*, a key element of the epigenetic machinery, as one of the targets of miR-137.

Materials and Methods

Cell lines and 5-aza-2-deoxy-cytidine treatment

We used six different CRC cell lines (HCT116, LoVo, RKO, SW48, HT29, and SW480) obtained from the American Type Culture Collection during the last 2 years. In our laboratory, all cells are tested and authenticated every 6 months using known genetic and epigenetic marks. Cells were grown in appropriate culture conditions. For demethylation experiments, cells were treated with 2.5 μmol/L 5-aza-2-deoxy-cytidine (5-aza-CdR; Sigma) for 72 hours, replacing the drug and medium every 24 hours.

Tissue specimens

A collection of 409 colorectal tissues were analyzed in this study, which included 113 sporadic primary CRCs with their corresponding adjacent normal colonic mucosa (N-C) and 68 colorectal adenomas obtained from the Okayama University Hospital, Okayama, Japan. Twenty-one normal colonic mucosa specimens from nontumor patients (N-N) were collected at the Hospital Clinic of Barcelona, Spain. Additionally, 47 CRC tissues and the corresponding adjacent normal mucosa from 11 patients with Lynch syndrome, 14 patients with microsatellite unstable CRCs, and 22 patients with microsatellite stable tumors were collected at Baylor University Medical Center, Dallas, Texas. All patients provided written informed consent and the study was approved by the Institutional Review Boards of all participating institutions. Clinicopathologic data of the patients are presented in Table 1 and Supplementary Table S1.

RNA extraction

Total RNA extraction was undertaken using the miRVana RNA extraction kit and the RecoverAll kit (both from Ambion, Inc.) according to the manufacturer's instructions.

DNA methylation analysis

The DNA methylation status of the miR-137 CpG island was established by PCR analysis of bisulfite-modified genomic DNA (EZ DNA methylation Gold Kit, Zymo Research) using three different methods. First, methylation status was analyzed by bidirectional bisulfite sequencing of HCT116 and RKO cell lines. Second, we performed methylation-specific PCR (MSP) using primers for either methylated or unmethylated DNA in the six CRC cell lines used in the study. Finally, we used bisulfite pyrosequencing for quantitative methylation analysis (PSQ HS 96A pyrosequencing system, QIAGEN). The primers used are described in Supplementary Table S2.

Table 1. Clinicopathologic features of colorectal cancer patients analyzed for miR-137 methylation

	Whole cohort (*n* = 113)	miR-137 unmethylated (*n* = 21)	miR-137 methylated (*n* = 92)	*P*
Age, mean (SD)	64.88 (11.17)	60 (14.1)	66 (10)	0.024*
Age >65, *n* (%)	59 (52.2)	9 (42.9)	50 (54.3)	0.342†
Female, *n* (%)	47 (41.6)	7 (33.3)	40 (43.5)	0.395†
Proximal location, *n* (%)‡	32 (28.3)	7 (35)	25 (27.2)	0.483†
MSI, *n* (%)	1 (0.9)	0 (0)	1 (1.1)	1†
KRAS mutation, *n* (%)	37 (32.7)	3 (14.3)	34 (37)	0.046†
BRAF mutation, *n* (%)	4 (3.5)	0 (0)	4 (4.3)	1†
Poorly differentiated adenocarcinoma, *n* (%)‡	9 (8)	3 (15)	6 (6.5)	0.2†
Mucinous adenocarcinoma, *n* (%)‡	5 (4.5)	3 (15)	2 (2.2)	0.039†
TNM‡				
I	14 (12.5)	3 (15)	11 (12)	0.713†
II	34 (30.4)	5 (25)	29 (31.5)	0.565†
III	43 (38.4)	5 (25)	38 (41.3)	0.174†
IV	21 (18.8)	7 (35)	14 (15.2)	0.057†

*Evaluated with Student's *t* test.
†Evaluated with χ^2 test or Fisher's exact test.
‡Results refer to 112 patients.

Analysis of miRNA expression using TaqMan reverse transcription-PCR

Expression of mature miR-137 was analyzed using the TaqMan miRNA Assay (Applied Biosystems, Inc.). Expression of RNU6B (Applied Biosystems) was used as an endogenous control. All the experiments were done in triplicate.

In situ hybridization

The *in situ* detection of miR-137 was performed on 5-μm formalin-fixed, paraffin-embedded (FFPE) sections from five normal colonic mucosa tissues, three adenomatous polyps, and five colorectal adenocarcinomas. Briefly, the slides were hybridized with 10 pmol probe (LNA-modified and DIG-labeled oligonucleotide; Exiqon) complementary to miR-137 and after incubation with anti–DIG-AP Fab fragments conjugated to alkaline phosphatase, and the hybridized probes were detected by applying nitroblue tetrazolium/5-bromo-4-chloro-3-indolyl phosphate color substrate (Roche) to the slides. Positive controls (RNU6B, Exiqon) and no-probe controls were included for each hybridization procedure.

Transfection of miR-137 precursor molecules

HCT116 cells were transfected with pre-miR miRNA precursor molecules (Ambion) or pre-miR miRNA negative control #1 (Ambion) at a final concentration of 100 nmol/L, using Lipofectamine 2000 (Invitrogen) according to the manufacturer's instructions. For microarray and reverse transcription-PCR (RT-PCR) analysis, total RNA was extracted 48 hours after transfection; for Western blot analysis, cell lysates were prepared 48 hours after transfection. To ensure transfection efficiency, we verified the protein downregulation of cyclin-dependent kinase 6 (CDK6), a previously validated target by Western blotting.

Gene expression microarray analysis, RT-PCR, and miRNA target prediction

HCT116 cells were transfected with control miRNA precursor or miR-137 precursor as described above. Extracted RNA was amplified using the Illumina TotalPrep RNA Amplification Kit. RNA integrity was assessed using the Agilent 2100 Bioanalyzer. Labeled cRNA was hybridized overnight to Human HT-12 V3 chips, washed, and scanned on an Illumina BeadStation-500. Illumina BeadStudio version 3.1 was used to process signal intensity values from the scans and background subtracted. Normalization was done using quantiles with the Lumi R-package. Fold changes were calculated with respect to their respective control. miRecords (http://mirecords.umn.edu/miRecords; ref. 15) was used to predict the miRNA targeting of miR-137. To narrow down the list of predicted targets, genes found to be downregulated (>2-fold change) after transfection of miR-137 precursor in the microarray were crossed with the genes predicted to be targets based on miRecords. Genes previously found to be associated with either CRC specifically or carcinogenesis in general were selected for validation.

For RT-PCR, RNA was reverse transcribed to cDNA from 1 μg of total RNA using random hexamers and Advantage RT-for PCR Kit (Clontech Laboratories). Power SYBR Green (Applied Biosystems) RT-PCR was performed for selected targets found with the strategy described above. Results were normalized to the expression of β-actin. All the experiments were performed in triplicates. Primer sequences are listed in Supplementary Table S2.

Western blot analysis

Western blot analysis was carried out using standard methods. The following primary antibodies were used: anti-CDK6 (Cell Signaling) at 1:2,000 dilution; anti-LSD1 (Cell Signaling) at 1:250 dilution; anti-SEMA4D (BD Transduction Laboratories) at 1:250 dilution; anti-AURKA (Cell Signaling) at 1:250 dilution; anti-CSE1L (BD Transduction Laboratories) at 1:1,000; anti-BX1 (Cell Signaling) at 1:1,000 dilution; and anti–β-actin antibody (Clone AC-15) at 1:32,000 dilution.

Luciferase reporter assay

Luciferase constructs were made by ligating oligonucleotides containing the wild-type or mutant putative target site of the *LSD1* 3′-untranslated region (UTR) downstream of the luciferase gene in the pMIR Reporter Luciferase vector (Ambion). Primers are detailed in Supplementary Table S2. Cells were cotransfected using Lipofectamine 2000 (Invitrogen) with 400 ng of firefly luciferase reporter vector containing the wild-type or mutant oligonucleotides, 200 ng of pGal control vector (Ambion), and 50 pmol of either miR-137 or negative control precursor. The parental luciferase plasmid was also transfected as a control. Luciferase activity was measured 48 hours after transfection (Bright Glo Luciferase Assay System, Promega) using β-galactosidase for normalization (β-galactosidase Enzyme Assay System, Promega). Experiments were performed in triplicate in three independent experiments.

Bromodeoxyuridine proliferation assay

The proliferation index was measured by bromodeoxyuridine (BrdUrd) incorporation in colon cancer cells 96 hours after transfection of either control miRNA precursor or miR-137 precursor as described above (Cell Proliferation ELISA, BrdUrd, Roche), following the manufacturer's instructions. Experiments were performed in triplicate in three independent experiments.

Statistical analysis

All data were analyzed using the SPSS 13 and GraphPad Prism 4.0 statistical software. Quantitative variables were analyzed using Student's test, Wilcoxon test (nonparametric paired analysis), and Mann-Whitney *U* test (nonpaired analysis). Qualitative variables were analyzed using χ^2 test or Fisher's exact test. A two-sided *P* value of <0.05 was regarded as significant.

Results

miR-137 is epigentically silenced in CRC cell lines

To determine the DNA methylation status in the miR-137 CpG island, we used a sequential approach. The CpG island of miR-137, along with the localization of PCR products for

each approach, is represented in Fig. 1A. First, we performed direct bisulfite sequencing of the promoter region of miR-137 in HCT116 and RKO cell lines, and we found extensive methylation throughout its promoter region in both cell lines, which was reversible following 5-aza-CdR treatment (Fig. 1C). Second, using MSP, we found that the miR-137 CpG island was extensively methylated in all of the CRC cell lines, and as expected, treatment with 5-aza-CdR induced significant demethylation (Fig. 1B). Third, we performed methylation analysis of miR-137 CpG island by quantitative pyrosequencing (Figs. 1D and 2A). Methylation, when present, generally affected all four sites CpG sites homogeneously; thus, their average was taken as the final measurement for analysis. The average methylation levels in HCT116, LoVo, RKO, SW48, HT29, and SW480 cells were 83%, 28%, 79%, 73%, 79%, and 29%, respectively.

We next analyzed the expression of miR-137 in the same panel of CRC cell lines using TaqMan RT-PCR, and we found an inverse correlation between the degree of CpG island methylation measured by pyrosequencing and the level of expression (Fig. 2A and B). Along with demethylation, treatment with 5-aza-CdR induced upregulation of miR-137 in CRC cell lines, suggesting that the expression of miR-137 is suppressed through CpG island promoter methylation in the majority of CRC cell lines.

Epigenetic silencing of miR-137 is an early event in colorectal carcinogenesis

We next used the miR-137 pyrosequencing assay to analyze the methylation status in a cohort of colorectal cancer tissues that included 21 normal mucosa from nontumor patients (N-N), 113 CRC tissues with their corresponding

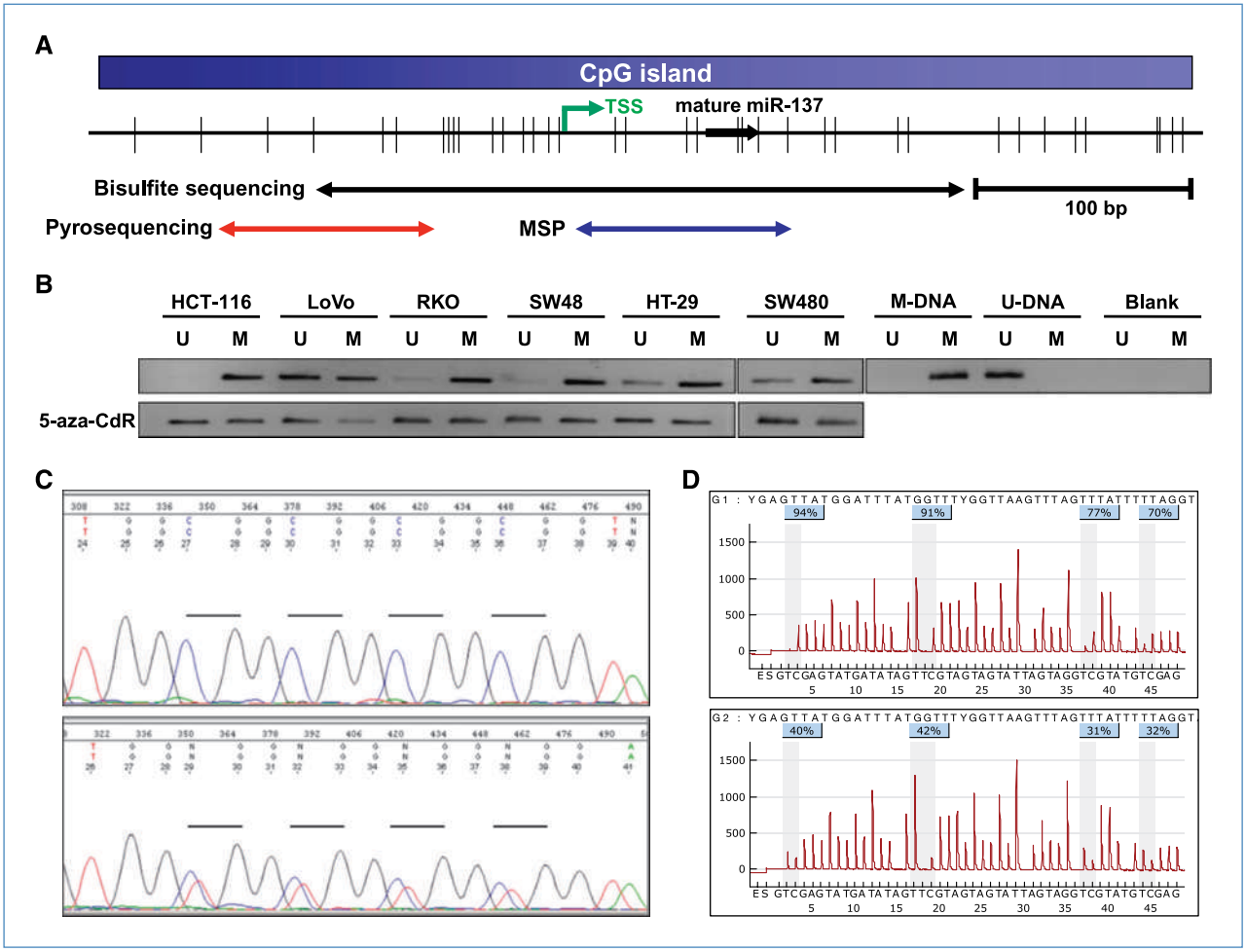

Figure 1. Methylation analysis of miR-137 CpG island. A, map of miR-137 CpG island, with the positions of mature miR-137 and PCR products used for methylation analysis indicated. Orange box, miR-137 CpG island; vertical tick marks, CpG sites. TSS, putative transcription start site. B, MSP analyses for miR-137 methylation in CRC cell lines. U, unmethylated state; M, methylated state; U-DNA, normal lymphocytes; M-DNA, *in vitro* methylated DNA. Top, parental cell lines. Bottom, analysis after 5-aza-CdR treatment. C, electropherogram corresponding to the bisulfite sequencing of four CpG sites in the HCT116 cell line. Top, parental cell lines. Bottom, methylation analysis after 5-aza-CdR treatment. Horizontal lines, CpG sites. D, results of bisulfite pyrosequencing of miR-137 in HCT116. Methylation percentages of four CpG sites (marked within gray vertical boxes) are indicated in the pyrogram. Top, parental cell lines with high levels of miR-137 methylation. Bottom, miR-137 demethylation after 5-aza-CdR treatment.

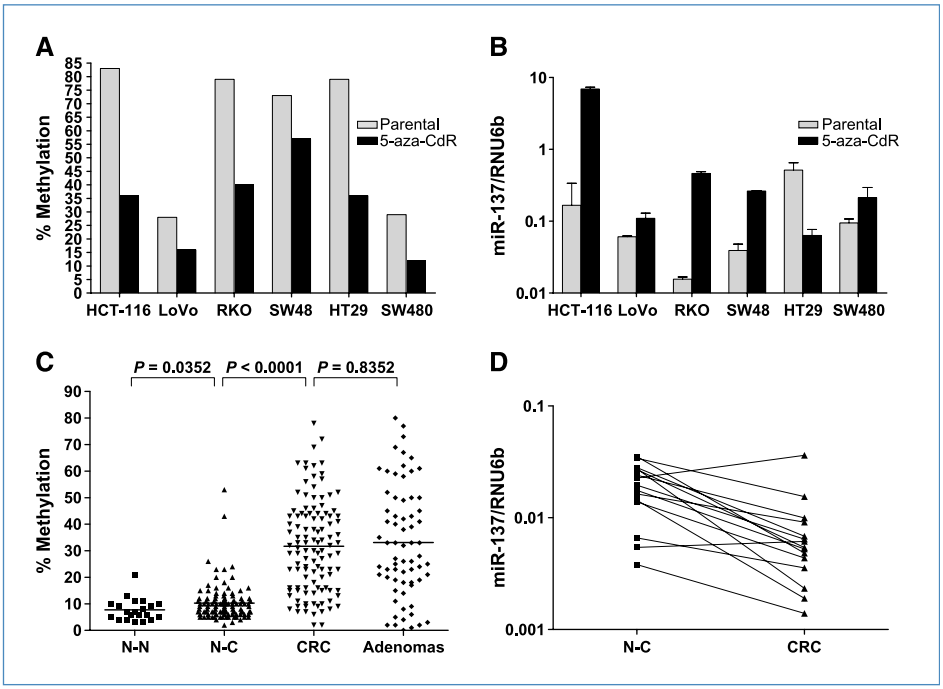

Figure 2. Methylation and expression analyses of miR-137 CpG island in CRC cell lines and in CRC tissues. A, bisulfite pyrosequencing results of miR-137 in six CRC cell lines. B, TaqMan RT-PCR analysis of miR-137 expression in CRC cell lines. Results are expressed as $2^{-\Delta\Delta Ct}$ (log_{10}) and normalized to RNU6b. Bars, SD. C, bisulfite pyrosequencing results of miR-137 in colorectal tissues: N-N (n = 21), N-C (n = 111), CRC (n = 113), and adenomas (n = 68). Black horizontal bar, mean methylation level. D, TaqMan RT-PCR analysis of miR-137 expression in 15 paired CRC tissues and N-C. Results are expressed as $2^{-\Delta Ct}$ and normalized to RNU6b.

adjacent normal mucosa (N-C), and 68 colorectal adenomas. The mean level of methylation (±SD) in N-N, N-C, CRC, and adenomas was 7.70% (±4.18), 10.27% (±6.88), 31.67% (±17.25), and 33.09% (±21.06), respectively (Fig. 2C). Thus, the level of methylation was significantly higher in CRC tissues compared with their corresponding histologically normal mucosa (31.67% versus 10.27%, $P < 0.0001$), showing the cancer specificity of miR-137 methylation. In addition, the level of miR-137 methylation in N-N or N-C did not correlate with older age (data not shown). On the other hand, we observed a significantly higher degree of methylation in N-C compared with N-N (10.2% versus 7.7%, $P = 0.0352$), consistent with the paradigm of methylation-related field defects in CRC. Finally, and more interestingly, methylation of miR-137 in adenomatous tissues showed the same degree of methylation as CRC tissues ($P = 0.8352$), suggesting that methylation of this miRNA is an early event in colorectal carcinogenesis.

To determine whether miR-137 methylation might be different among the different molecular subtypes of CRC based on the presence of microsatellite instability (MSI), we next analyzed miR-137 methylation status in tumors and matching normal tissues (N-C) from 11 patients with Lynch syndrome, 14 patients with sporadic MSI, and 22 MSS patients. The mean levels of methylation in Lynch, sporadic MSI, and MSS were 22%, 27.3%, and 24.7%, respectively. The corresponding levels in N-C were 6.4%, 6.2%, and 7.3%, respectively. Accordingly, miR-137 methylation seems to be equally present in all molecular subtypes of CRC.

Because pyrosequencing analysis allows quantitative measurements, we next analyzed miR-137 methylation results as a categorical variable. We determined a methylation cutoff based on the average miR-137 methylation levels in normal mucosa from nontumor individuals plus 2 SD (cutoff, 15%). Based on these results, miR-137 was methylated in 4% (1 of 21) of N-N, 14.4% (16 of 111) of N-C, 81.4% (92 of 113) of CRC, and 82.3% (56 of 68) of adenomas. Clinicopathologic features of CRC and adenoma patients are listed in Table 1 and Supplementary Table S1, respectively. Patients with CRC-associated miR-137 methylation were significantly older than those without methylation (66 versus 60 years-old, $P = 0.024$), showed more frequent somatic *KRAS* mutations (37% versus 14.3%, $P = 0.046$), and were less frequently associated to mucinous features (2.2% versus 15%, $P = 0.039$). There was no association between methylation status and TNM stage. In adenoma patients, we observed a significantly higher degree of methylation in villous compared with nonvillous adenomas (44.28% versus 29.08%, $P = 0.0051$).

miR-137 is constitutively expressed in the colonic epithelium and downregulated in CRC

We used TaqMan RT-PCR to assess the expression of miR-137 in 15 pairs of CRC and normal colonic mucosa and found substantial downregulation of the expression in the tumor compared with the normal mucosa (Fig. 2D). Interestingly, the only two cases that did not show downregulation in the tumor tissue were those not associated with methylation (data not shown).

To investigate which specific cell types expressed miR-137 in the colon, we performed *in situ* hybridization using 5′-DIG–labeled LNA probes, a technique that has been applied to the detection of miRNA *in situ* in FFPE tissues (Fig. 3). In normal colonic mucosa, miR-137 was expressed only in the colonic epithelial cells throughout the colonic crypts. However, none of the adenomatous and CRC samples showed miR-137 expression, consistent with our observation that miR-137 is silenced in the majority of colonic neoplastic tissues.

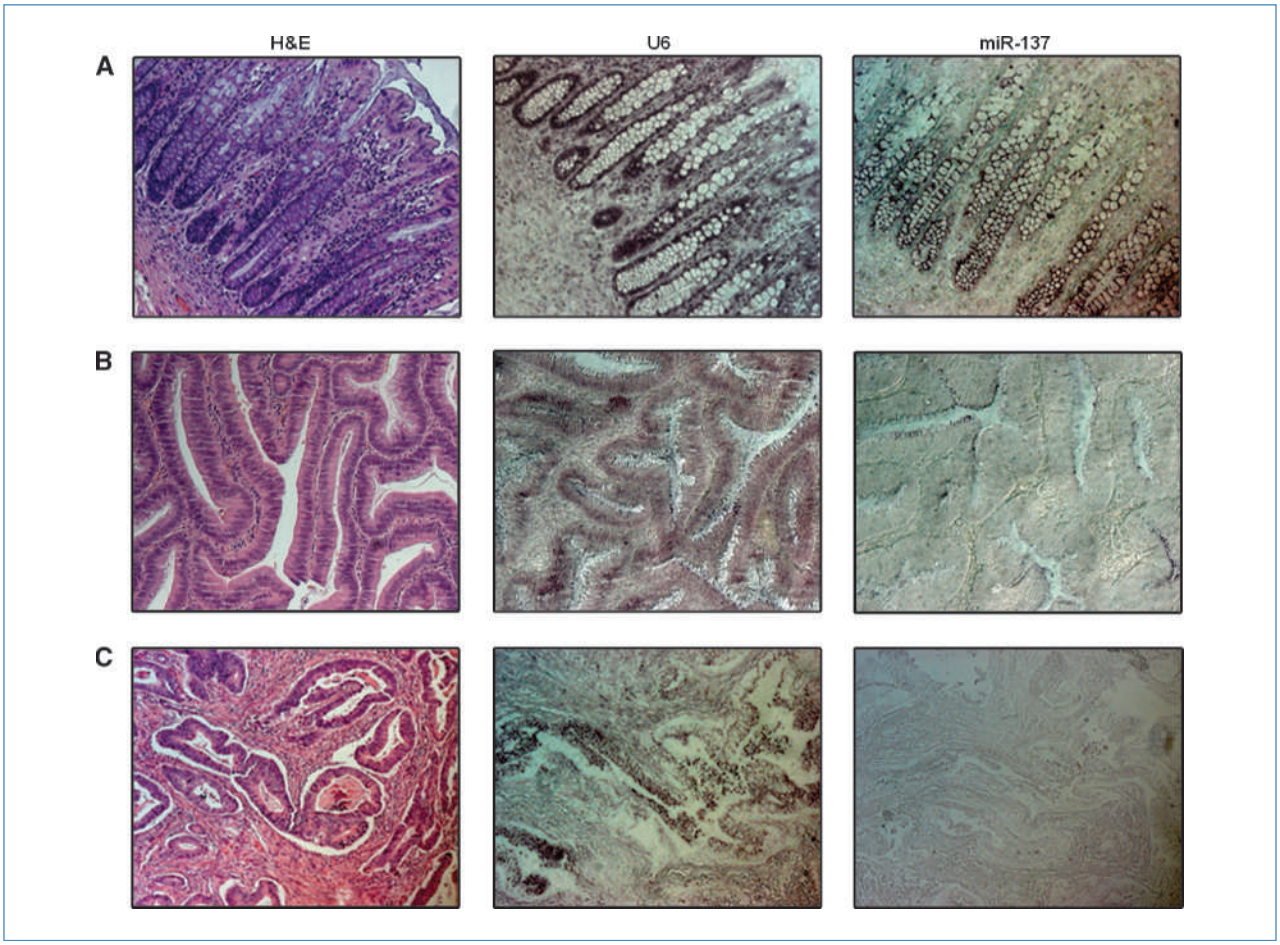

Figure 3. *In situ* hybridization analysis of miR-137 in normal colorectal mucosa and CRC. miR-137, positive control (U6), and negative control (no probe) *in situ* hybridization analyses were performed in normal colorectal mucosa (A) and a group of adenomas (B) and CRC (C). Staining for miR-137 was observed in the epithelium throughout the colonic crypt, with no staining of the stromal cells. However, miR-137 was not expressed in any of the neoplastic tissues evaluated. H&E staining of the corresponding tissues is shown.

miR-137 transfection inhibits cell proliferation

Having discovered that miR-137 is epigenetically silenced in CRC through CpG island methylation, we next performed functional studies to determine whether miR-137 had *in vitro* tumor-suppressive features following transfection of miR-137 precursor into CRC cell lines. We performed BrdUrd incorporation assays after transfection of either miR-137 precursor or a negative control precursor in three different colon cancer cell lines. Restoration of miR-137 significantly reduced cell proliferation in HCT116 and RKO but not in SW480 (Fig. 5D), suggesting the specificity of miR-137 as a tumor suppressor in CRC.

Identification of potential gene targets of miR-137

To identify gene targets of miR-137, we first performed whole genome gene expression analysis in HCT116 cells after transfection of either miR-137 or negative control precursors. Four hundred ninety-one genes showed more than 2-fold decrease in their expression following miR-137 transfection, compared with the negative controls (Supplementary Table S3). We next used the miRecords resource (15) to obtain a list of predicted miR-137 targets. This bioinformatics approach integrates information of predicted miRNA targets produced by 11 established miRNA target prediction programs, thus providing a more accurate and comprehensive assessment of predicted targets compared with a single database. Selecting the predicted targets from at least 4 of the 11 prediction tools included in the website, we obtained a list of 505 potential targets (Supplementary Table S3). After cross-referencing the list of miR-137–related gene targets from our own gene expression microarray data and information gathered from the miRecords database, we determined that 32 genes met the criteria of downregulation by miR-137 transfection and being an *in silico* predicted target (Fig. 4A and B).

We first validated the microarray data by RT-PCR (Fig. 4C) for a subset of selected genes. Lysine (K)-specific demethylase 1A (KDM1A; also known as *LSD1*), chromosome segregation 1-like (*CSE1L*), Y box binding protein 1 (*YBX1*), semaphorin 4D (*SEMA4D*), and Aurora Kinase A (*AURKA*) were chosen for validation because of their putative role in

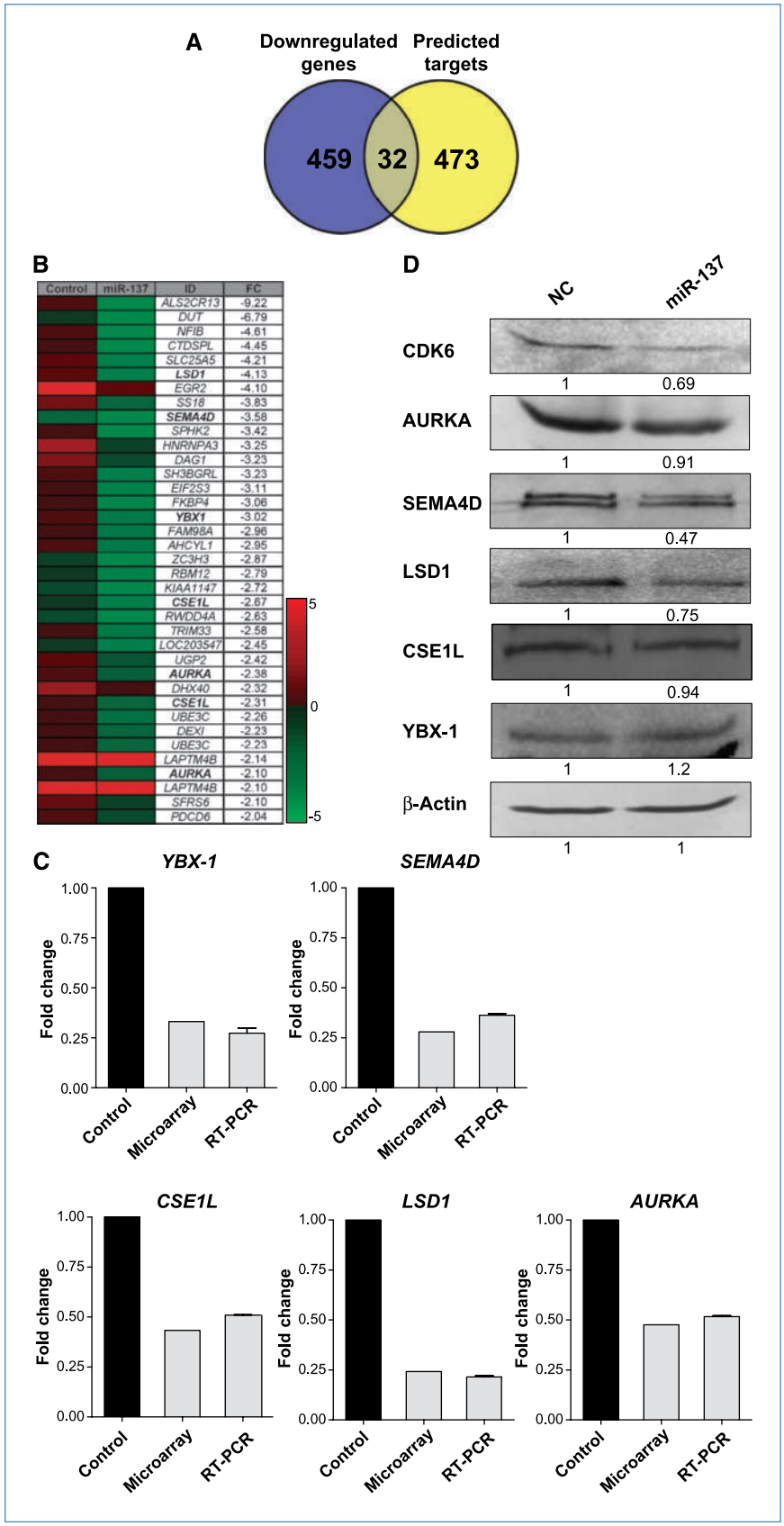

Figure 4. Identification of potential targets of miR-137 in CRC. A, the Venn diagram represents the downregulated genes (≥2-fold change) observed in the gene expression microarray analysis after transfection of miR-137 precursor (in blue) and the predicted targets generated by the *in silico* prediction tool miRecords (in yellow). B, list of genes identified using the mentioned strategy. The expression intensity of each mRNA varies from red (above average) to green (below average). ID, gene name; FC, fold change. C, comparison between the quantitative RT-PCR and microarray results. For each gene, the variation in expression compared with control is represented as average fold change for both the microarray and the quantitative RT-PCR analysis (bars, SD). D, Western blot analysis of potential miR-137 targets. Densitometric analysis of protein expression is shown below each blot, in relation to NC and normalized to β-actin expression.

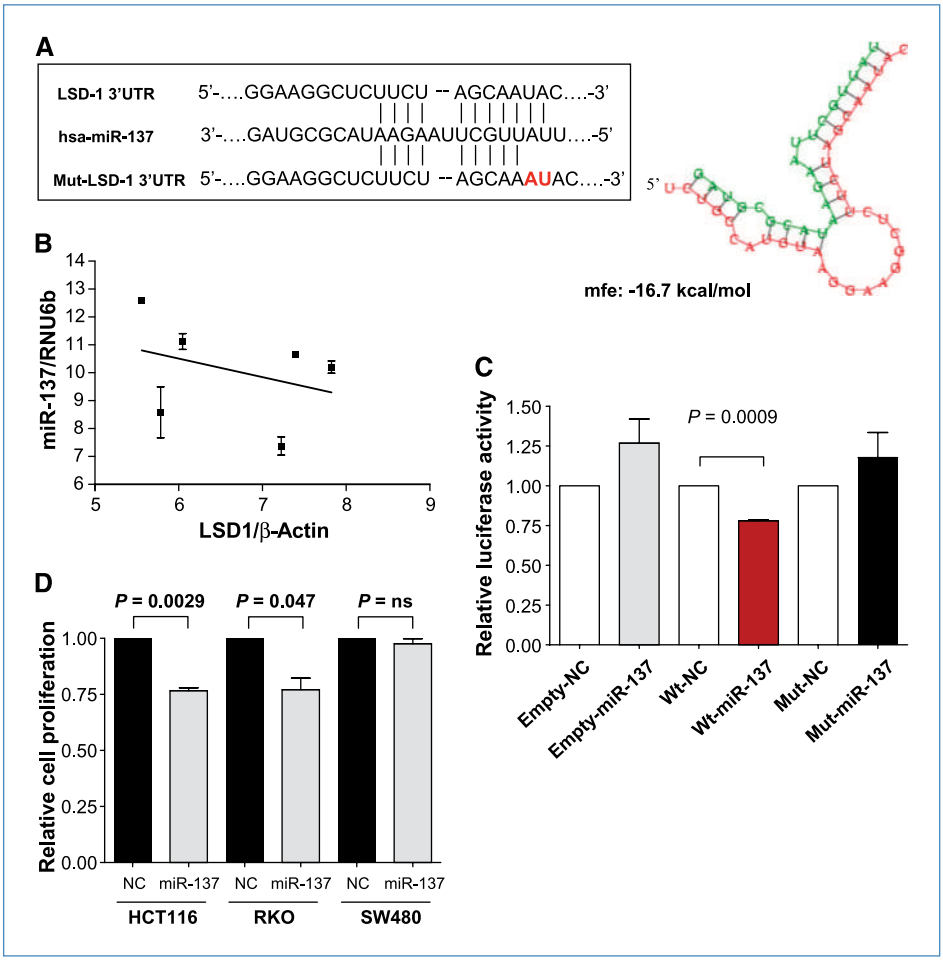

Figure 5. Interaction between miR-137 and *LSD1* and tumor suppressor features of miR-137. A, the predicted hybridization of miR-137 (green) with the 3′UTR region of *LSD1* mRNA (red) using RNAhybrid software. The minimum free energy (mfe) required for RNA hybridization is shown. The conserved predicted binding site of miR-137 with the 3′UTR region of *LSD1* mRNA is also represented. The mutated binding site used for the luciferase assay is shown in red. B, correlation between miR-137 expression and *LSD1* mRNA levels across a panel of six CRC cell lines. Results are expressed as $2^{-\Delta Ct}$. RNU6b and β-actin were used for normalization. Bars, SD. C, direct recognition of *LSD1* mRNA 3′UTR by miR-137. Luciferase assay of HCT116 cells transfected with firefly luciferase constructs containing *LSD1*-mut or *LSD1*-wt. The parental luciferase plasmid (empty) was also transfected as a control. β-Galactosidase activity was calculated for normalization. Bars, SD. D, effect of miR-137 on cell proliferation (BrdUrd assay). Bars, SD.

carcinogenesis. Sequence interaction between the 3′UTR region of these genes and miR-137 is shown in Supplementary Fig. 1. RT-PCR results were highly concordant with microarray data for all selected genes. All of these genes contain well-conserved target sites in their 3′UTR region for miR-137, and Western blot analysis effectively showed different degrees of downregulation of expression in three of five selected genes after miR-137 precursor transfection (Fig. 4D).

LSD1 is a direct target of miR-137

We next explored the functional interaction between miR-137 and *LSD1* (Fig. 5A–C). The expression levels of miR-137 and *LSD1* mRNA were determined in six CRC cell lines by TaqMan RT-PCR and RT-PCR, respectively (Fig. 5B). In CRC cell lines with lower endogenous miR-137 expression (HCT116, LoVo, RKO, and SW48), a higher *LSD1* expression level was observed, whereas in the HT29 cell line, which has higher expression levels of miR-137, the amount of *LSD1* was much lower.

To determine if the 3′UTR region of *LSD1* was indeed a functional target site of miR-137, a luciferase reporter plasmid harboring either wild-type or mutated predicted region of interaction at the *LSD1* 3′UTR region was constructed. The transient transfection of HCT116 cells with the wild-type reporter plasmid and the miR-137 precursor led to a decrease of luciferase activity in comparison with the control precursor (Fig. 5C). However, the luciferase activity remained unaffected following transfection with either the parental plasmid or the one with the mutated sequence.

Discussion

In this study, we report that epigenetic silencing through promoter methylation of miR-137 is an early event in colorectal carcinogenesis. *In situ* hybridization analysis showed that this miRNA is constitutively expressed in the normal colonic epithelium and is silenced in neoplastic tissues. Gene expression analysis combined with *in silico* prediction tools allowed us to identify several potential targets of miR-137, including *LSD1*, a histone demethylase that plays a central role in the epigenetic machinery.

Our data indicate that methylation of the miR-137 promoter is an early event in colorectal carcinogenesis, supported by the fact that the average methylation level in adenomas was similar to that in CRC specimens (31.67% versus 33.09%, respectively; $P = 0.8352$). In addition, miR-137 methylation seems to be tumor specific because it preferentially occurs in neoplastic tissues and its methylation in normal colonic

mucosa did not increase as a function of age. More interestingly, we found a higher degree of average methylation in histologically normal colorectal mucosa from CRC patients compared with the normal mucosa from nontumor patients (10.27% versus 7.7%, respectively; $P = 0.0352$), consistent with the epigenetic field defect proposed in CRC (16). The rationale for this phenomenon relies on the fact that sporadic CRCs are thought to arise from a region of cells characterized by a "field defect" (17). DNA methylation of multiple genes has been proposed as a major contributor to the field defect hypothesis (16); however, only two previous studies have suggested that miRNA methylation may have an analogous manifestation in the gastrointestinal tract. Grady and colleagues found that miR-342, an intronic miRNA encoded within the *EVL* gene, was methylated in 56% of normal-appearing colonic mucosa from CRC patients and in six of nine adenomas (10). In gastric cancer, Ando and colleagues recently found that methylation of miR-124a1-3 shows a similar pattern in the normal gastric mucosa from tumor and healthy subjects (18). We must mention that tissue specimens for normal colonic mucosa from CRC patients and healthy subjects were obtained from two different populations from Japan and Spain, respectively. Consequently, the differences in miR-137 methylation in these tissues could be attributed to other factors, such as ethnicity or other environmental factors that require further analysis to definitively establish the field defect associated with miR-137 methylation in the colon. Based on our findings for cancer specificity, the high level of methylation in colonic adenomas, and the potential field defect feature, the methylation status of miR-137 may serve as a potential noninvasive biomarker for CRC.

Although several studies have shown that miRNA expression profiles in CRC are significantly different than the normal colonic mucosa, it is unclear which specific cell types within the colon express various miRNAs. Elucidation of this aspect is essential to our understanding of the biological function of miRNAs in carcinogenesis, as these are known to have different roles in different cell types, and the same miRNA can act as a tumor suppressor or an oncogene depending on the tissue and cell compartment (2). *In situ* hybridization in FFPE tissues has been recently used for miRNA detection with great success for different cancers (19). We found that miR-137 is preferentially expressed in the epithelial cells of normal colonic mucosa, whereas no miR-137 expression was observed in any of the adenomatous polyps and CRC tissues. These findings are of significance and are consistent with our gene expression data that showed downregulation of miR-137 in CRC relative to normal mucosa.

Given the evidence that miR-137 is commonly silenced in CRC cell lines and CRC tissues due to promoter methylation, we performed functional studies to explore the potential tumor suppressor features of miR-137 *in vitro*. We discovered that the restoration of miR-137 expression in HCT116 and RKO cells, two cell lines with lower constitutive miR-137 expression, indeed resulted in a significant decrease in proliferation. Although further studies are needed, our results suggest that miR-137 may act as a tumor suppressor miRNA in CRC.

A critical and challenging step in understanding miRNA function is the identification of its gene targets. Lack of reliable and specific methods for target identification limits our understanding of the biological role of miRNAs. Computational methods, the most commonly used approach, are based on base pairing between the miRNA seed region (first 2–8 bases of the mature miRNA) and the target, but suffer from specificity issues because predicted targets are usually in the hundreds or thousands, making it difficult to ascertain the authentic targets of a given miRNA. Whereas miRNAs were believed to act mainly through translational inhibition rather than mRNA cleavage, it is increasingly being realized that miRNAs may downregulate a much larger number of transcripts than previously appreciated (7, 20, 21). Thus, gene expression microarray analysis has been proposed as a useful strategy to identify physiologically relevant miRNA:mRNA interactions. In this study, candidate miR-137 targets were selected using a combination of bioinformatic and transcriptomic approaches. We used stringent criteria to decrease the false positivity rate and identified 32 potential targets that were downregulated after miR-137 transfection at the mRNA level. These same gene targets were also predicted targets by at least four of the available computational-based prediction tools. It was encouraging to observe that our protein expression analysis revealed that three of the five selected genes also showed corresponding downregulation of protein expression following miR-137 transfection, thus reinforcing the value of this strategy.

Interestingly, we found that *LSD1*, a histone demethylase, is a target of miR-137. *LSD1* is part of a new class of histone demethylating enzymes that, in addition to demethylating H3K4 and H3K9 (22, 23), are essential for the maintenance of global DNA methylation through demethylation of a nonhistone substrate, DNMT1, by increasing its stability (24). Because many human cancers show increased expression of DNMT1, it is plausible to speculate that *LSD1*, which is often upregulated in cancer cells, might be partly responsible for this epigenetic defect. Overexpression of *LSD1* has been documented in prostate cancer (22) and in neuroblastoma (25), where *LSD1* is involved in maintaining the undifferenciated phenotype and inhibition of its function inhibits tumor xenograft growth. In line with this argument, we found an inverse correlation between miR-137 and *LSD1* in CRC cell lines and validated this functional interaction using luciferase experiments. Because *LSD1* seems to play a central role in the epigenetic machinery and has a potential role in cancer therapy (26), future experiments will reveal additional roles of *LSD1* in CRC carcinogenesis and its relationship with modulation of miR-137 expression.

In summary, this study reports that miR-137 acts a tumor suppressor in the colon and is frequently silenced in CRC through promoter hypermethylation and that its restoration inhibits cell proliferation *in vitro*. Because miR-137 methylation is an early event in colorectal carcinogenesis, the potential use of miR-137 methylation as a CRC biomarker is very promising. We have identified multiple potential

mRNA targets of miR-137, including *LSD1* in CRC, which provides novel evidence for the cross-talk between miRNAs and other components of the epigenetic machinery. These findings raise the possibility that in the future, miR-137 precursors may have potential therapeutic value in CRC patients.

Disclosure of Potential Conflicts of Interest

No potential conflicts of interest were disclosed.

Grant Support

National Cancer Institute, NIH, grants R01 CA72851 and CA129286 and funds from the Baylor Research Institute (C.R. Boland and A. Goel), Fundación Alfonso Martín Escudero (F. Balaguer), and Societat Catalana de Digestologia (F. Balaguer).

The costs of publication of this article were defrayed in part by the payment of page charges. This article must therefore be hereby marked *advertisement* in accordance with 18 U.S.C. Section 1734 solely to indicate this fact.

Received 02/22/2010; revised 06/01/2010; accepted 06/09/2010; published OnlineFirst 08/03/2010.

References

1. Lu J, Getz G, Miska EA, et al. MicroRNA expression profiles classify human cancers. Nature 2005;435:834–8.
2. Calin GA, Croce CM. MicroRNA signatures in human cancers. Nat Rev Cancer 2006;6:857–66.
3. Lanza G, Ferracin M, Gafa R, et al. mRNA/microRNA gene expression profile in microsatellite unstable colorectal cancer. Mol Cancer 2007;6:54.
4. Schetter AJ, Leung SY, Sohn JJ, et al. MicroRNA expression profiles associated with prognosis and therapeutic outcome in colon adenocarcinoma. JAMA 2008;299:425–36.
5. Doleshal M, Magotra AA, Choudhury B, Cannon BD, Labourier E, Szafranska AE. Evaluation and validation of total RNA extraction methods for microRNA expression analyses in formalin-fixed, paraffin-embedded tissues. J Mol Diagn 2008;10:203–11.
6. Lujambio A, Ropero S, Ballestar E, et al. Genetic unmasking of an epigenetically silenced microRNA in human cancer cells. Cancer Res 2007;67:1424–9.
7. Toyota M, Suzuki H, Sasaki Y, et al. Epigenetic silencing of microRNA-34b/c and B-cell translocation gene 4 is associated with CpG island methylation in colorectal cancer. Cancer Res 2008;68:4123–32.
8. Croce CM. Causes and consequences of microRNA dysregulation in cancer. Nat Rev Genet 2009;10:704–14.
9. Bandres E, Agirre X, Bitarte N, et al. Epigenetic regulation of microRNA expression in colorectal cancer. Int J Cancer 2009;125:2737–43.
10. Grady WM, Parkin RK, Mitchell PS, et al. Epigenetic silencing of the intronic microRNA hsa-miR-342 and its host gene EVL in colorectal cancer. Oncogene 2008;27:3880–8.
11. Lujambio A, Esteller M. CpG island hypermethylation of tumor suppressor microRNAs in human cancer. Cell Cycle 2007;6:1455–9.
12. Bemis LT, Chen R, Amato CM, et al. MicroRNA-137 targets microphthalmia-associated transcription factor in melanoma cell lines. Cancer Res 2008;68:1362–8.
13. Kozaki K, Imoto I, Mogi S, Omura K, Inazawa J. Exploration of tumor-suppressive microRNAs silenced by DNA hypermethylation in oral cancer. Cancer Res 2008;68:2094–105.
14. Silber J, Lim DA, Petritsch C, et al. miR-124 and miR-137 inhibit proliferation of glioblastoma multiforme cells and induce differentiation of brain tumor stem cells. BMC Med 2008;6:14.
15. Xiao F, Zuo Z, Cai G, Kang S, Gao X, Li T. miRecords: an integrated resource for microRNA-target interactions. Nucleic Acids Res 2009;37:D105–10.
16. Shen L, Kondo Y, Rosner GL, et al. MGMT promoter methylation and field defect in sporadic colorectal cancer. J Natl Cancer Inst 2005;97:1330–8.
17. Ushijima T. Epigenetic field for cancerization. J Biochem Mol Biol 2007;40:142–50.
18. Ando T, Yoshida T, Enomoto S, et al. DNA methylation of microRNA genes in gastric mucosae of gastric cancer patients: its possible involvement in the formation of epigenetic field defect. Int J Cancer 2009;124:2367–74.
19. Schepeler T, Reinert JT, Ostenfeld MS, et al. Diagnostic and prognostic microRNAs in stage II colon cancer. Cancer Res 2008;68:6416–24.
20. Lim LP, Lau NC, Garrett-Engele P, et al. Microarray analysis shows that some microRNAs downregulate large numbers of target mRNAs. Nature 2005;433:769–73.
21. Chen X, Guo X, Zhang H, et al. Role of miR-143 targeting KRAS in colorectal tumorigenesis. Oncogene 2009;28:1385–92.
22. Metzger E, Wissmann M, Yin N, et al. LSD1 demethylates repressive histone marks to promote androgen-receptor-dependent transcription. Nature 2005;437:436–9.
23. Shi Y, Lan F, Matson C, et al. Histone demethylation mediated by the nuclear amine oxidase homolog LSD1. Cell 2004;119:941–53.
24. Wang J, Hevi S, Kurash JK, et al. The lysine demethylase LSD1 (KDM1) is required for maintenance of global DNA methylation. Nat Genet 2009;41:125–9.
25. Schulte JH, Lim S, Schramm A, et al. Lysine-specific demethylase 1 is strongly expressed in poorly differentiated neuroblastoma: implications for therapy. Cancer Res 2009;69:2065–71.
26. Huang Y, Stewart TM, Wu Y, et al. Novel oligoamine analogues inhibit lysine-specific demethylase 1 and induce reexpression of epigenetically silenced genes. Clin Cancer Res 2009;15:7217–28.